Is the law of optical reflection true?

Tom A. Kuusela*

Department of Physics and Astronomy,

University of Turku, 20014 Turku, Finland

(Dated: January 27, 2026)

Abstract

The reflection of light from a dielectric interface follows well-known optical principles, such as the equality of the angles of incidence and reflection, as well as Snell's law of refraction. These laws hold precisely when considering the behavior of a single plane wave at an optical interface. However, real optical beams, which have finite spatial and angular extents, exhibit deviations from these idealized laws. Specifically, reflected beams can undergo spatial displacements and angular deflections, collectively referred to as beam shifts. The Goos–Hänchen shift displaces the beam in a direction perpendicular to the plane of incidence, while the Imbert–Fedorov shift introduces a transverse displacement for circularly polarized light. These effects arise from the angular dispersion of the reflection coefficients and from the spin-orbit interaction of circularly polarized light. These shifts can be described using classical electromagnetism; however, this paper presents the theory behind these shifts using a highly compact quantum mechanical formulation. The shifts are small, only a fraction of the wavelength of light. By applying the weak measurement technique known from quantum mechanics, these shifts can be significantly enhanced. We introduce an experimental setup that allows such amplified shifts to be easily measured, even in student laboratories.

I. INTRODUCTION

It has long been known that the angle of reflection is equal to the angle of incidence. A proof of this can be found in any optics textbook, along with the well-known Snell's laws of refraction. These proofs are perfectly valid when considering a single plane wave and its reflection from a surface. However, in reality, such a situation never occurs, as a single plane wave, being infinitely large in spatial extent, is unphysical.

It is much less well known, and rarely presented in textbooks, that a beam with finite angular aperture, does not strictly obey the simple laws of reflection or refraction.[1,2] When such a light beam is reflected, it can experience various spatial displacements and angular deflections.[3–5] The first such beam shift was discovered by Goos and Hänchen in 1943 for totally internally reflected linearly polarized light.[6–8] In this GH shift, the center of the light beam is slightly displaced in the plane of incidence, i.e., longitudinally (see Fig. 1(a)). If the incident light has circular polarization, a transverse Imbert–Fedorov (IF) shift occurs (see Fig. 1(b)).[9] These shifts and their corresponding angular deflections are generic, meaning they can occur in almost any optical system, and they also appear in refraction.

The physical explanation of the GH effect is related to the dispersion of the reflection and refraction coefficients, meaning that they depend on the beam's angle of incidence.[7] The propagation of a physical light beam cannot be described by a single wave vector; instead, it consists of a distribution of wave vectors around the central one. Each wave-vector component of the beam is therefore reflected or refracted slightly differently. The IF phenomenon, on the other hand, is fundamentally related to the conservation of the angular momentum of light, including the intrinsic spin associated with circular polarization and the spin-orbit interaction of light.[10] The IF effect is closely related to the spin Hall effect of light.[11] If the incident light is linearly polarized, as it is in our experiments, it can be described as a superposition of left- and right-circularly polarized components. These polarization components experience equal but opposite IF shifts (see Fig. 2). However, there is no net transverse shift for the overall beam. The polarizations associated with the plane-wave components of the beam undergo different rotations to satisfy transversality after reflection. As a result, the reflected beam acquires a weakly inhomogeneous polarization, as shown in the insets of Fig. 2.[11]

The GH and IF beam shifts, which are largest in total internal reflection and near the

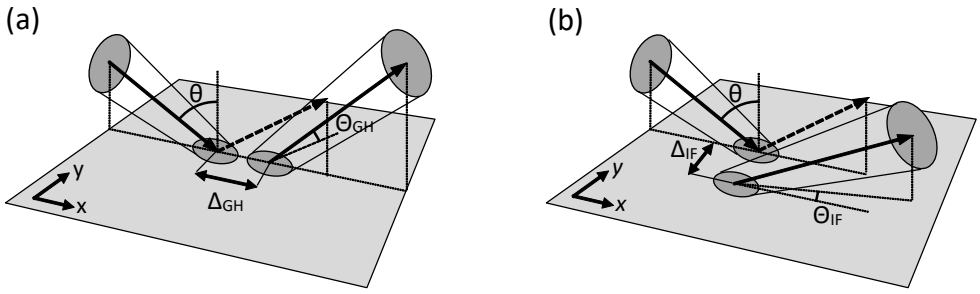

FIG. 1: (a) Longitudinal in-plane Goos–Hänchen (GH) shifts occurring upon reflection of a bounded beam from a planar surface. The deviation from the ray optics prediction consists of the spatial Δ_{GH} and angular Θ_{GH} shifts. (b) Transversal Imbert–Fedorov (IF) shifts. The deviation from the ray optics prediction consists of the spatial Δ_{IF} and angular Θ_{IF} shifts. θ is the incidence angle of the beam.

critical angle, are usually very small — only a fraction of the wavelength of light — making them quite difficult to measure. The angular deflections of the beams are proportional to the square of beam's angular divergence, and are typically only on the scale of microradians. In the original work, Goos and Hänchen measured the beam shift by allowing linearly polarized light to undergo total internal reflection dozens of times in succession within a glass plate.[6] As a reference path, they used another beam traveling through the same glass plate, but instead of encountering a glass-air interface, it reflected from a glass-metal interface. After multiple reflections, they observed a small difference in the exit positions of the two beams. The IF shift, however, cannot be measured in this way, as consecutive total internal reflections would cancel each other out. Instead, Imbert directed circularly polarized light to propagate appropriately along a prism and ultimately measured the difference relative to a reference beam.[9]

GH and IF shifts can be significantly enhanced using a method known from quantum mechanics, namely the so-called weak measurement technique. This method was first applied in measurements of the spin Hall effect of light.[11] In this context, weak measurement is not related to the quantum nature of light but can be understood as a purely classical way to describe the measurement process.[12,13] With weak measurement, the shifts and corresponding angular deflections typically produce beam deviations on the order of tens of micrometers, making it possible to perform experiments even in student laboratories.

In Section II, we present the main theoretical results of optical beam shifts within the

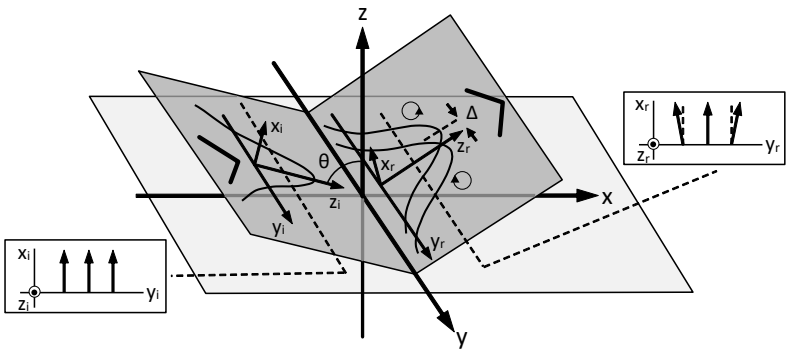

FIG. 2: Spin Hall effect of light in the IF shift. The input horizontal polarization state $|H\rangle = \frac{1}{\sqrt{2}}(|R\rangle + |L\rangle)$ (along x_i) splits to strongly overlapping right and left circularly polarized states in the IF shift after reflection. The edges of the reflected beam are not strictly horizontally polarized as shown in the inserts.

mathematical framework of quantum mechanics, which allows for a highly compact representation. In Section III, we discuss the experimental setup and provide practical guidelines. Finally, in Section IV, we present GH and IF measurement results for both total internal and partial external reflection.

II. THEORY

It is well known that the paraxial wave equation, widely used in optics, is formally equivalent to the Schrödinger equation for the free propagating of a quantum particle, with time replaced by path length.[13,14] Therefore, we can describe an optical beam with polarization as the wave function of a nonrelativistic particle with spin 1/2. It should be emphasized that this correspondence is purely formal, and no quantum character of the electromagnetic field is taken into account. All calculations of beam reflection and refraction can be done classically in terms of electromagnetic theory[12] but the quantum mechanical description provides a convenient way derive essential results in a very compact way. Here, we do not repeat all computational steps but instead present only the minimal set of results that can be directly used to calculate various types of beam shifts at an optical interface.[3,5,13].

Let ket vector $|\psi(z)\rangle$ represent the solution $\psi(x, y, z)$ of the paraxial-wave equation. We can recover $\psi(x, y, z) = \langle \hat{\boldsymbol{R}}|\psi(z)\rangle$ where $\hat{\boldsymbol{R}}$ is the transversal position operator $\{\hat{x}, \hat{y}\}$. The complete state including the polarization is given by $|\Psi(z)\rangle = |\psi(z)\rangle|A\rangle$ where $|A\rangle$ is a

two-component spinor $\{a_p, a_s\}$ representing the p (parallel to the plane of incidence) and s (orthogonal to plane of incidence) polarizations of the input beam, with the normalization requirement $|a_p|^2 + |a_s|^2 = 1$.[14] The displacement of the centroid of the Gaussian beam distribution after reflection, with respect to the centroid of the reflected beam found using the simple geometric optics, is given by the expectation value

$$\langle \boldsymbol{R} \rangle(z) = \frac{\langle \Psi(z)|\hat{\boldsymbol{R}}|\Psi(z)\rangle}{\langle \Psi(z)|\Psi(z)\rangle} = \frac{1}{k}\,\mathrm{Re}\,\frac{\langle A_F|\hat{\boldsymbol{A}}|A_F\rangle}{\langle A_F|A_F\rangle} + \frac{1}{k}\frac{z}{L}\,\mathrm{Im}\,\frac{\langle A_F|\hat{\boldsymbol{A}}|A_F\rangle}{\langle A_F|A_F\rangle}. \tag{1}$$

The vector $|A_F\rangle$ is $\{r_p a_p, r_s a_s\}$ corresponding to the initial spinor after simple Fresnel reflection. The matrix valued spin-operator $\hat{\boldsymbol{A}} = \{\mathrm{X}, \mathrm{Y}\}$ where the matrices X and Y are the following:

$$\mathrm{X} = \begin{bmatrix} -i\dfrac{1}{r_p}\dfrac{\partial r_p}{\partial \theta} & 0 \\ 0 & -i\dfrac{1}{r_s}\dfrac{\partial r_s}{\partial \theta} \end{bmatrix}, \mathrm{Y} = \begin{bmatrix} 0 & i\dfrac{1}{r_s}(r_p + r_s)\cot(\theta) \\ -i\dfrac{1}{r_p}(r_p + r_s)\cot(\theta) & 0 \end{bmatrix}, \tag{2}$$

where $r_s(\theta) = R_s \exp(i\phi_s)$ and $r_p(\theta) = R_p \exp(i\phi_p)$ are the complex reflection coefficients, and θ the incidence angle of the beam. The coordinate z is the distance from the waist of the beam, the parameter $L = \pi\omega_0^2/\lambda$ the Rayleigh range, ω_0 the beam waist, $k = 2\pi/\lambda$ the wavenumber and λ the wavelength.

The first term in (1), the real part of the expectation value of $\hat{\boldsymbol{A}}$, represents the spatial shift of the beam, while the last term, the imaginary part, corresponds to the angular shift; that is, a shift in wave-vector space. Actually, an imaginary value means shift in the space of the wave vectors. This latter term enables the utilization of beam-propagation enhancement of the shifts, as it increases with the distance z from the beam waist. However, increasing the distance also increases the diameter of the beam and thereby reduces the maximum intensity and thus weakens the signal-noise ratio, making it difficult to perform accurate measurements.

From Eqs. (2) we can immediately see some basic properties. For example, if the incident beam is vertically polarized ($a_s = 1$, $a_p = 0$) and total internal reflection occurs ($R_s = 1$), the term $\langle A_F|\,\mathrm{X}\,|A_F\rangle$ is proportional to the derivative $d\phi_s/d\theta$. This shows that such a shift is fundamentally related to the dispersion of light: in the angular spectrum of the incident beam, the components incident at different angles are reflected with slightly different amplitudes and phases, and the resulting interference manifests as an average displacement of the reflected beam.

On the other hand, for any linearly polarized beam, $\langle A_F|\,\mathrm{Y}\,|A_F\rangle = 0$, meaning that no shift occurs. Only when the incident beam is circularly (or, in general, elliptically) polarized do we obtain a nonzero shift associated with the operator Y. This, in turn, indicates that the angular momentum of light plays an essential role in this phenomenon.

By using the matrices (2) in Eq. (1), we obtain (see also Figs. 1(a) and 1(b))

$$\begin{aligned} \Delta_{\mathrm{GH}} &= \frac{1}{k}\,\mathrm{Re}\,\frac{\langle A_F|\mathrm{X}|A_F\rangle}{\langle A_F|A_F\rangle}, \quad \Theta_{\mathrm{GH}} = \frac{1}{kL}\,\mathrm{Im}\,\frac{\langle A_F|\mathrm{X}|A_F\rangle}{\langle A_F|A_F\rangle}, \\ \Delta_{\mathrm{IF}} &= \frac{1}{k}\,\mathrm{Re}\,\frac{\langle A_F|\mathrm{Y}|A_F\rangle}{\langle A_F|A_F\rangle}, \quad \Theta_{\mathrm{IF}} = \frac{1}{kL}\,\mathrm{Im}\,\frac{\langle A_F|\mathrm{Y}|A_F\rangle}{\langle A_F|A_F\rangle}. \end{aligned} \tag{3}$$

If the reflection coefficients $r_s(\theta)$ and $r_p(\theta)$ are known, the spatial and angular shifts in Eq. (3) can be immediately calculated as functions of the incidence angle θ. It is important to note that neither of the matrices X or Y is Hermitian; consequently, their expectation values need not be real and may, in general, be complex. Thus, they do not directly corresponds to a measurable physical quantity. It is also noteworthy that neither of shifts Δ_{GH} or Δ_{IF} depends on the spatial characteristics of the beam, but solely on the material properties via the Fresnel coefficients. This is valid only for a fundamental Gaussian beam. When the beam possesses spatial structure, such as in high-order Laguerre-Gauss beams carrying orbital angular momentum, additional contributions to the shifts arise. Finally, the angular shifts Θ_{GH} and Θ_{IF} scale inversely with L. In the limit of an infinitely large beam waist, $L \to \infty$, and these shifts vanish. This limiting case corresponds to a plane wave, which possesses no angular spread.

All the shifts in Eq. (3) are typical quantum mechanical expectation values of an operator in the usual von Neumann sense, given by the form $\langle A\rangle = \langle\psi_i|A|\psi_i\rangle/\langle\psi_i|\psi_i\rangle$ where the degrees of freedom of the measured system are traced over by taking inner products with the initial state $|\psi_i\rangle$ and normalized by $\langle\psi_i|\psi_i\rangle$. However, instead of this expectation value, we can consider the projection of the measured system onto a certain post-selected final state $|\psi_f\rangle$. In this case, we obtain the weak value of the operator $\langle A_w\rangle = \langle\psi_f|A|\psi_i\rangle/\langle\psi_f|\psi_i\rangle$.[4,15,16] The weak value is usually complex and can take on very large values when the $|\psi_i\rangle$ and $|\psi_f\rangle$ are nearly orthogonal. Weak measurements can be applied to significantly enhance beam shifts in certain situations. In practice, this can be achieved by placing a polarizer in front of the detector, aligned along the direction $|B\rangle = \{b_s, b_p\}$, where $|b_s|^2 + |b_p|^2 = 1$. Now, we

can express the post-selected and weak-valued versions of the shifts (3)

$$\begin{aligned} \Delta^{w}_{\mathrm{GH}} &= \frac{1}{k}\,\mathrm{Re}\,\frac{\langle B|\mathrm{X}|A_F\rangle}{\langle B|A_F\rangle}, \quad \Theta^{w}_{\mathrm{GH}} = \frac{1}{kL}\,\mathrm{Im}\,\frac{\langle B|\mathrm{X}|A_F\rangle}{\langle B|A_F\rangle}, \\ \Delta^{w}_{\mathrm{IF}} &= \frac{1}{k}\,\mathrm{Re}\,\frac{\langle B|\mathrm{Y}|A_F\rangle}{\langle B|A_F\rangle}, \quad \Theta^{w}_{\mathrm{IF}} = \frac{1}{kL}\,\mathrm{Im}\,\frac{\langle B|\mathrm{Y}|A_F\rangle}{\langle B|A_F\rangle}. \end{aligned} \tag{4}$$

Normally in quantum mechanics, a weak measurement means that we have a pointer system which interacts weakly on the system under study. Here we have an interaction between the polarization and the spatial structure of the beam, and weakness come out from the beam paraxiality.

In the following experimental works, we use these post-selected GH and IF shifts in various configurations. For example, if the input polarization state is $|A\rangle = |V\rangle$ (and thus $|A_F\rangle = r_s|V\rangle$), we can set the post-selection state $|B\rangle = \cos(\epsilon)|H\rangle + \sin(\epsilon)|V\rangle$ where the parameter ϵ can be adjusted by rotating the polarizer in front of the camera. It should be noted that although linearly polarized light does not experience any average IF shift of the beam, the situation is different when weak measurements are performed in the manner described above. In that case, we measure small inhomogeneities in polarization of the reflected light (see Fig. 2).

III. EXPERIMENTAL SETUP

The experimental setup is shown in Fig. 3. As a light source, we use a He-Ne laser with a wavelength 633 nm, a power 0.5 mW, a beam aperture 240 μm and linear polarization. The laser's intrinsic waist is not critical, since it can always be tailored to the desired value with a suitable focusing lens. The polarization state of the laser beam is set using a Glan–Thompson calcite polarizer (Thorlabs GTH5M) mounted on a precision rotation mount (Thorlabs PRM05). If the output beam of the laser is linearly polarized, a half-wave plate (HWP) should be placed before the first polarizer in order to maximize the light intensity after that. A positive lens with a focal length of 100 mm determines the spot size ω_0 of the Gaussian beam and its position.

Although the waist and position can be calculated based on the properties of the laser beam, these parameters are often not well known. Therefore, it is preferable to measure the beam waist directly using a digital camera. We measured the size and position of the waist

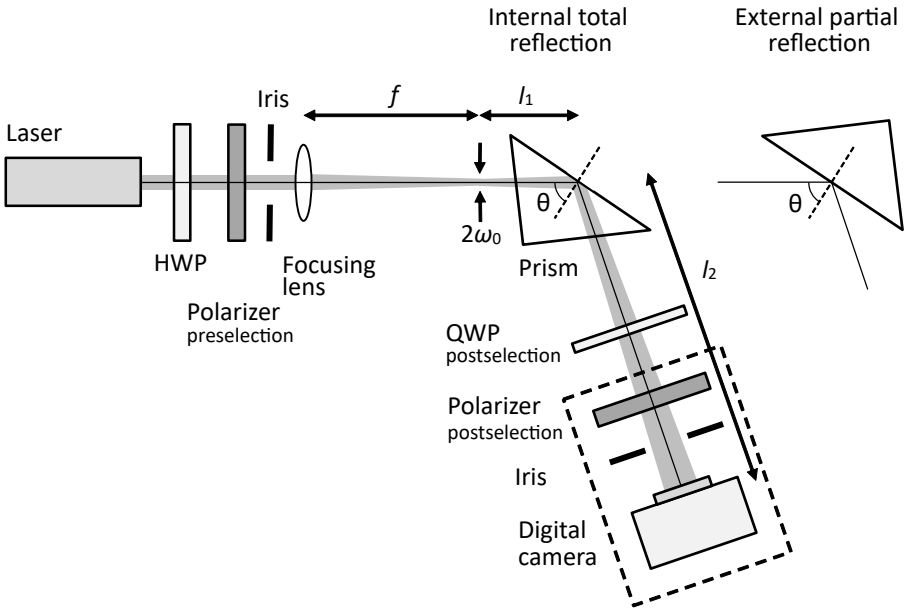

FIG. 3: Setup of the optical measurement system for the cases of internal total and external partial reflection. The half-wave plate (HWP) is used to maximize the beam intensity. The polarization of the laser beam is set by a polarizer. The focusing lens determines the position (approximately at the focal length from the lens) and the diameter $2\omega_0$ of the beam waist. The polarization state of the reflected beam is post-selected by the quarter-wave plate (QWP; used only in one experiment) and another polarizer. The distance from the beam waist to the digital camera is $z = l_1 + l_2$.

by translating the camera and searching the minimum waist. In our setup, the measured waist ω_0 is 89 μm.

The 45°–90°–45° BK7 glass prism (Thorlabs PS910, refractive index $n = 1.52$) is mounted on a rotation platform (Thorlabs RP01). The prism can be configured either for the total internal reflection or partial external reflection. The reflected beam is analyzed using another Glan–Thompson polarizer mounted on a precision rotation mount with micrometer adjustment (Thorlabs PRM1) and a digital camera (IDS UI-1242L, 1280×1024 pixels, area 6.784 mm $\times$ 5.427 mm). The post-selection polarizer, the iris and the camera are mounted on a separate plate to keep them mutually aligned. The distance $z = l_1 + l_2$ from the beam waist to the camera sensor is fixed at 124 mm ($l_1 = 24$mm, $l_2 = 100$ mm). It is possible to use a second collimating lens placed before the detector to ensure that the detector's distance does not affect the measurement results. However, in this setup, this is not necessary as long as the distance is kept constant, and because an additional lens may introduce other

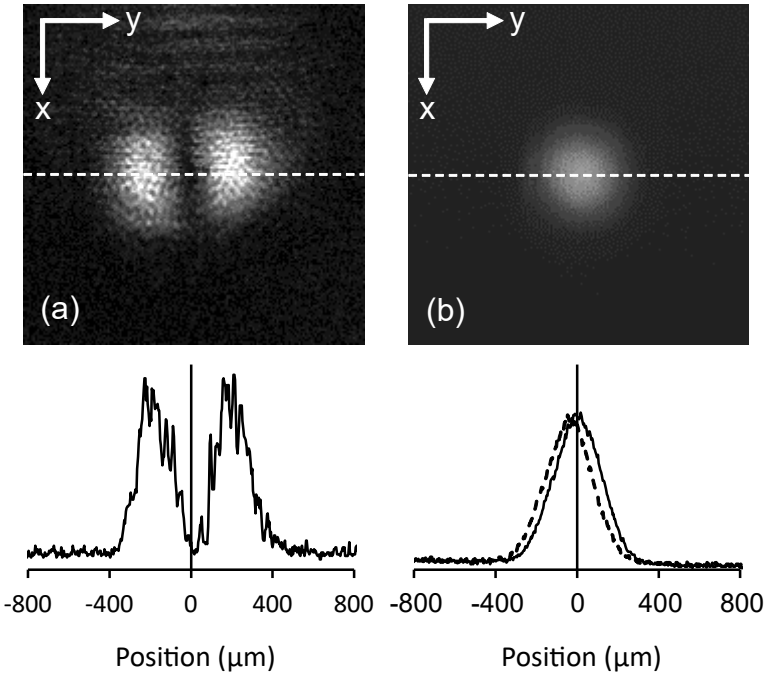

FIG. 4: Camera images of the light beam after total reflection and the corresponding intensity distribution measured along the dashed line. The x and y coordinates correspond to the coordinates x_r and y_r in Fig. 2. Note that y coordinate is in the horizontal direction of the images for clarity. (a) Pre- and post-selection polarizers are orthogonal to each other ($\epsilon = 0$; see Eq. (4) and the text after). (b) The weak measurement condition: $\epsilon = +1^\circ$ (solid line) or $\epsilon = -1^\circ$ (dashed line). The actual light intensity in (b) is 200 times higher than in (a).

issues, it is preferable not to include it.

It should be noted that focusing the beam on the reflection interface is not necessary. The beam waist can be located either before or after the interface, as only the distance to the detector is relevant in the angular deflection.[11] This fact may seem counterintuitive. The actual angular deflection does indeed occur at the reflective interface, but the overall effect can be interpreted such that the dielectric interface acts as a kind of virtual image at the incident beam waist. This phenomenon is not unique to the fundamental Gaussian beam but applies (at least to first order) also to other spatial beam profiles. In the quantum mechanical description, this feature manifests in the fact that the free propagation operator of the beam and the interaction operator commute, meaning their order can be interchanged.

We found that moderate beam-propagation enhancement z/L values (< 10) are preferable, as a short focal length of the focusing lens and a small beam waist (Rayleigh range L

is proportional with ω_0^2) easily lead to a non-Gaussian beam shape, unwanted interference effects, and, consequently, difficulties in accurately measuring beam shifts. Glan-Thompson polarizers are excellent due to their high extinction ratio, which is especially important in the postselection stage. However, the non-transmitted part of the beam is not absorbed by the polarizer but instead reflected off the calcite crystals and only partially absorbed by the black aluminum mounting tube. The scattered light can significantly reduce the contrast of the camera images. Therefore, irises are mounted just after both polarizer to reduce background illumination. Glan–Taylor polarizers (such as Thorlabs GT5 with the SM05PM5 mount) can also be used, where the transmitted ordinary ray exits through a side window, which largely mitigate problems associated with backscattered beam. However, these polarizers exhibit a significantly limited field of view — only a few degrees — in contrast to approximately 40° for a Glan–Thompson type making alignment more challenging.

In the literature, beam shifts are typically measured using quadrant detectors. We observed that a digital camera is highly useful, as it allows simultaneous measurement of both the beam shape and its position. The intensity distribution is fitted with a Gaussian function, and the beam's central position is determined with an accuracy of approximately 3 μm, slightly better than the pixel size. An example of the camera output with the s input polarization and total reflection producing IF shift is shown in Fig. 4(b). The difference between the beam's central positions is 42 μm, corresponding to postselection rotation angles of $\epsilon = \pm 1^\circ$ for the polarizer. The actual IF shift is half of this, or 21 μm.

When the polarizers are crossed, the previous results for the beam shifts are no longer valid, as $\epsilon = 0$. This situation must therefore be analyzed separately. In turns out that the transmitted beam is no longer Gaussian beam but instead exhibits a double-peak intensity profile, as shown in Fig. 4(a).[17,18] The distance between the peaks is approximately $\sqrt{2}\omega$, where ω is the beam waist expected at the camera's position. In our example, $\omega = 310$ μm, leading to a predicted peak separation of 440 μm, which is quite close to the observed distance of 420 μm. This double peak phenomenon becomes more intuitive when we revisit Fig. 2. After reflection of the originally horizontally polarized beam, the beam edges acquire a small vertical polarization component. The crossed post-selection polarizer selectively transmits only these components.

The double-peak situation is highly sensitive to the rotation angles of the polarizers and is therefore extremely useful in experiments. When the double peaks are visible, we know that

polarizers are accurately crossed (or that the post-selection is orthogonal to pre-selection). This ensures that further post-selections in weak measurements are performed symmetrically around this zero condition. In practice, we first adjust both the post-selection polarizer (and possibly other optical elements, such as wave plates) and typically also fine-tune the pre-selection polarizer until two distinct peaks are clearly visible. After this adjustment, we can proceed with the actual weak measurements by slightly rotating the post-selection polarizer.

It is important to note that, although weak measurements can greatly enhance small shifts, the approach remains an approximation that breaks down as the post-selected state becomes nearly orthogonal to the initial state. In practice, this leads to a deformation of the beams transverse profile, which deviates from a Gaussian shape. Consequently, the shifts obtained through such measurements should be interpreted with appropriate caution.

IV. RESULTS

A. Imbert–Fedorov shift in total internal reflection

If we have vertical s input polarization ($a_s = 1$ and $a_p = 0$ or $|A\rangle = |V\rangle$), then according to Eqs. (4,) we obtain

$$X_s = \frac{\langle B|\mathrm{X}|A_F\rangle}{\langle B|A_F\rangle} = -\frac{i}{r_s}\frac{\partial r_s}{\partial \theta}, \quad Y_s = \frac{\langle B|\mathrm{Y}|A_F\rangle}{\langle B|A_F\rangle} = i\frac{b_p^*}{b_s^*}\left(1+\frac{r_p}{r_s}\right)\cot(\theta). \tag{5}$$

Clearly, the GH shift cannot be enhanced by weak measurement, as it does not depend on the post-selection polarization. Instead, an enhanced IF shift can be achieved.[18] If we use the post-selection polarization $|B\rangle = \cos(\epsilon)|H\rangle + \sin(\epsilon)|V\rangle$, we obtain

$$Y_s = i\cot(\epsilon)\left(1+\frac{r_p}{r_s}\right)\cot(\theta). \tag{6}$$

Y_s grows indefinitely as $\epsilon \to 0$.

In the case of total internal reflection, the complex reflection coefficients are given by $r_i = \exp(i\phi_i)$ ($i = s$ or p), leading to

$$i\left(1+\frac{r_p}{r_s}\right) = -\sin(\phi_p - \phi_s) + i[1+\cos(\phi_p - \phi_s)]. \tag{7}$$

Finally, we obtain the total IF beam shift:

$$\begin{aligned}\langle y\rangle_s &= \frac{1}{k}\cot(\epsilon)\cot(\theta)\left[\mathrm{Re}(Y_s) + \frac{z}{L}\,\mathrm{Im}(Y_s)\right] \\ &= \frac{1}{k}\cot(\epsilon)\cot(\theta)\left[-\sin(\phi_p-\phi_s) + \frac{z}{L}(1+\cos(\phi_p-\phi_s)\right].\end{aligned} \tag{8}$$

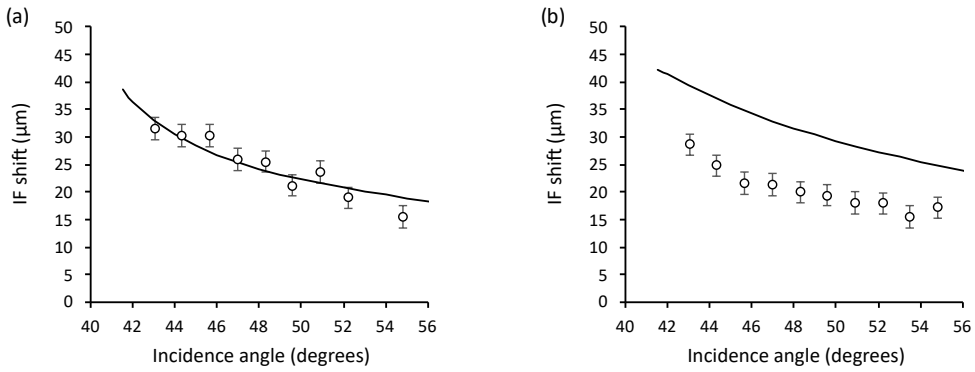

FIG. 5: (a) The IF shift in total internal reflection for the s-polarized input beam as a function of the incidence angle ($\epsilon = \pm 1^\circ$). The solid line represents the theoretical prediction. (b) Same as in (a) but for the p-polarized input beam.

The experimental result for the IF shift in total internal reflection with s input polarization as a function of the incidence angle is shown in Fig. 5(a). The Gaussian beam waist is 89 μm, the distance of the camera from the waist is $z = l_1 + l_2 = 124$ mm, the ratio z/L is 3.15 and the weak measurement parameter ϵ is $\pm 1^\circ$. With these settings, the enhancement factor for the spatial shift is $\cot(\epsilon) = 57$ and for the angular shift $\cot(\epsilon)(z/L) = 181$. Shifts are determined as a half of the difference between the measured beam positions corresponding to the polarizer angles $\pm 1^\circ$. We observe that the experimental transversal shifts are quite close to the theoretical predictions, and the longitudinal shifts are negligible. It should be noted that without the enhancement due to the beam propagation and weak measurement, the shifts would be only a few tens of nanometers and therefore very difficult to measure. The incidence angle at the glass-air interface is calculated from the rotation angle of the prism and "normal" refraction at the air-glass interface. Both IF and GH shifts at this interface are negligible since the incidence angle is close to zero.[11]

With p input polarization ($a_s = 0$ and $a_p = 1$ or $|A\rangle = |H\rangle$), we have a very similar situation to the case with s input polarization, as the GH shift cannot be enhanced by the weak measurement. Using the post-selection $|B\rangle = -\sin(\epsilon)|H\rangle + \cos(\epsilon)|V\rangle$), we have

$$Y_p = i \cot(\epsilon) \left(1 + \frac{r_s}{r_p}\right) \cot(\theta) \tag{9}$$

and correspondingly the total IF shift

$$\langle y \rangle_p = \frac{1}{k} \cot(\epsilon) \cot(\theta) [\sin(\phi_p - \phi_s) + \frac{z}{L}(1 + \cos(\phi_p - \phi_s)]. \tag{10}$$

The experimental results for p input polarization are shown in Fig. 5(b). The scattering of the data points appears to be quite small, but they deviate significantly from the theoretical prediction. Several repeated measurement could not explain this discrepancy. Interestingly, exactly same kind of results are reported in a previous study without any obvious explanation.[18] It is possible that the equations describing the shifts, Eq.(1) or Eq. (4), are no longer sufficiently accurate. They assume that the measurement is weak in the sense that the final state $\hat{\boldsymbol{A}}|A_F\rangle$ is largely undisturbed by the action of $\hat{\boldsymbol{A}}$.[5] In practice, this means that the beam's polarization state and shape do not change too much upon reflection. In our experiments, we observed that the beam imaged by the camera did not exhibit a perfectly Gaussian shape, which suggests that a higher-order analysis may be necessary. It is evident that this situation should be examined more closely.

B. Imbert–Fedorov shift in the partial external reflection

In the partial external reflection, the reflection coefficients $r_i = R_i$ are real. In this case, Y_s in Eq. (5) is purely imaginary. With s input polarization ($|B\rangle = \cos(\epsilon)|H\rangle + \sin(\epsilon)|V\rangle$), we obtain the total IF shift:

$$\langle y \rangle_s = \frac{1}{k}\frac{z}{L}\cot(\epsilon)\cot(\theta)\left(1 + \frac{R_p}{R_s}\right). \tag{11}$$

Experimental results for this type of IF shift as a function of the incidence angle are shown in Fig. 6(a). Experimental data are in reasonably good agreement with the theory, especially considering that we are quite close to the resolution limit of the camera setup. With p input polarization ($|B\rangle = -\sin(\epsilon)|H\rangle + \cos(\epsilon)|V\rangle$), the total IF shift is given by

$$\langle y \rangle_p = \frac{1}{k}\frac{z}{L}\cot(\epsilon)\cot(\theta)\left(1 + \frac{R_s}{R_p}\right). \tag{12}$$

In this case, R_p approaches zero at the Brewster angle (here 56.7°), leading to a singularity in the IF shift. Additionally, the sign of the shift changes below and above the Brewster angle.[19,20] The experimental results are displayed in Fig. 6(b). In practice, performing measurements near the Brewster angle is challenging due to the low beam intensity. However, the results are surprisingly close to the theoretical predictions.

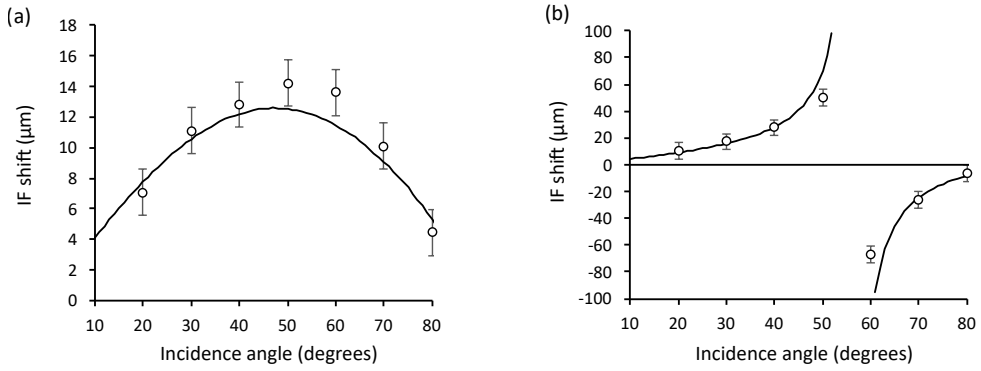

FIG. 6: (a) The IF shift in partial external reflection for the s-polarized input beam as a function of the incidence angle angle ($\epsilon = \pm 1^\circ$). The solid line represents the theoretical prediction. (b) Same as in (a) but for the p-polarized input beam.

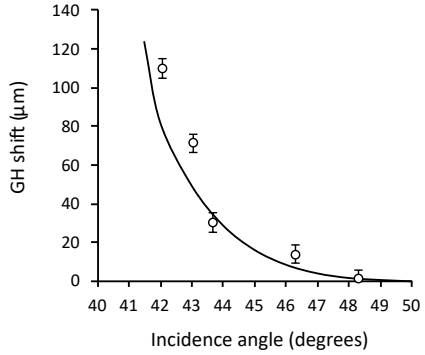

FIG. 7: The GH shift in total internal reflection for the diagonally polarized input beam as a function of the incidence angle angle ($\epsilon = 1^\circ$). The solid line represents the theoretical prediction.

C. Goos–Hänchen shift in the total internal reflection

A weak value enhancement of the GH shift is not possible if the input polarization is either s or p input polarization, as explained previously. However, with a diagonal input polarization ($a_s = a_p = 1/\sqrt{2}$), this type of enhancement can be utilized both in the total reflection[21,22] and in the partial reflection.[23] We perform experiments in the total reflection using the same setup as previous. When the input polarizer is set at the angle of $\pi/4$, the post-selection polarizer is set at $\pi/4+\pi/2\pm\epsilon$. Straightforward but lengthy calculation based on Eq. (5) yields the total GH shift

$$\langle x\rangle_d = \frac{1}{2k}\left\{\left(\frac{d\phi_p}{d\theta}+\frac{d\phi_s}{d\theta}\right) - \cot(\epsilon)\left[\cos(\phi_p+\phi_s)+\frac{z}{L}\sin(\phi_p+\phi_s)\right]\left(\frac{d\phi_p}{d\theta}-\frac{d\phi_s}{d\theta}\right)\right\}. \quad (13)$$

An analysis of the polarization state after the reflection reveals that the beam is not linearly polarized but slightly elliptical. The obvious reason for this is that s and p polarization components of the input beam experience a different, incidence-angle-dependent, phase shift (see Appendix D, Fig. 12(b)). Therefore, it is necessary to add a quarter-wave plate (QWP) before the post-selection polarizer. To ensure orthogonality between pre- and post-states, both the QWP and the post-selection polarizer (and often also slightly the pre-selection polarizer) must be carefully adjusted. This makes the experiments rather challenging. The experimental results with diagonal input polarization are shown in Fig. 7. As we can see, the GH shift increases rapidly when approaching the critical angle. In this case the transversal shifts are negligible.

D. Enhancement parameters

Finally, we examine how well the theoretical predictions regarding the essential effects — beam propagation and weak measurement enhancements — can be experimentally reproduced. We use total internal reflection with s input polarization as an example case.

First, the IF shift as a function of the weak measurement parameter ϵ is shown in Fig. 8. Comparing the theoretical predictions given by Eq. (8) with the measured shifts, we find excellent agreement, except at very small values of ϵ ($< 0.1°$) . In practice, the smallest useful value of ϵ is limited by the finite extinction rate of the polarizers. As we can see, it would be possible to increase the weak measurement enhancement by at least a factor of three compared to the chosen value of $\epsilon = 1°$. However, this would lead to a significant drop in intensity and, consequently, in the signal-to-noise ratio.

Second, we consider whether the IF shift increases linearly with the distance from the beam waist. Measurements confirm that this is largely true, as shown in Fig. 9, although some systematic deviations appear, particularly at smaller and possibly also at larger distances. This type of measurement can be employed to separate the spatial shifts (Δ_{GH} and Δ_{IF}) from the angular shifts (Θ_{GH} and Θ_{IF}). In the present case, fitting a regression line to the experimental data and extrapolating to zero distance yields $\Delta_{\mathrm{IF}} = -4$ μm, whereas the corresponding theoretical prediction is -7 μm.

Very long distances are not practical, but beam propagation enhancement can be increased by using a smaller beam waist while maintaining moderate waist distances. How-

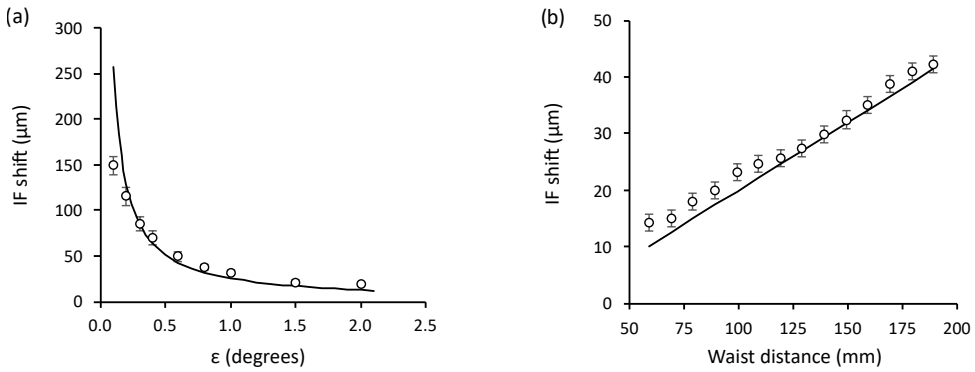

FIG. 8: (a) The IF shift (total internal reflection, s-polarisation, the incidence angle 46°, the waist distance 124 mm) as a function of ϵ. The solid line represents the theoretical prediction. (b) The IF shift (total internal reflection, s-polarisation, the incidence angle 46°, $\epsilon = 1°$) as a function of the waist distance. The solid line represents the theoretical prediction

ever, as in the previous case, a trade-off must be made between the signal-to-noise ratio and enhancement, as the beam waist at the detector increases rapidly. In previous studies, an enhancement factor as high as 10^4 has been reported but achieving this requires an extremely well-controlled measurement system.[11]

V. CONCLUDING REMARKS

It is truly fascinating that such a seemingly ordinary optical phenomenon as light reflection is, in reality, a remarkably complex and versatile physical event when considering an actual physical light beam rather than the idealized plane wave approach. For students, this serves as an example of how rich electromagnetic theory and its practical applications actually are.

Although the Goos–Hänchen and Imbert–Fedorov shifts are very small, they are present in virtually all optical devices involving a dielectric interface. However, similar optical shifts have also been observed in many other situations, such as with metals[24], optically active materials[25], multilayer structures[26], dissipative media[27], semiconductors[28], metamaterials[29], and photonic crystals.[30] The beam-shift effects are also sensitive to the shape of the incident beam. In addition to simple Gaussian beams, shifts are considered for structured light, such as higher-order Hermite-Gaussian beams[31] and beams carrying orbital angular momentum, like Laguerre-Gaussian beams.[32] And finally, the beam shift in reflection does not necessarily

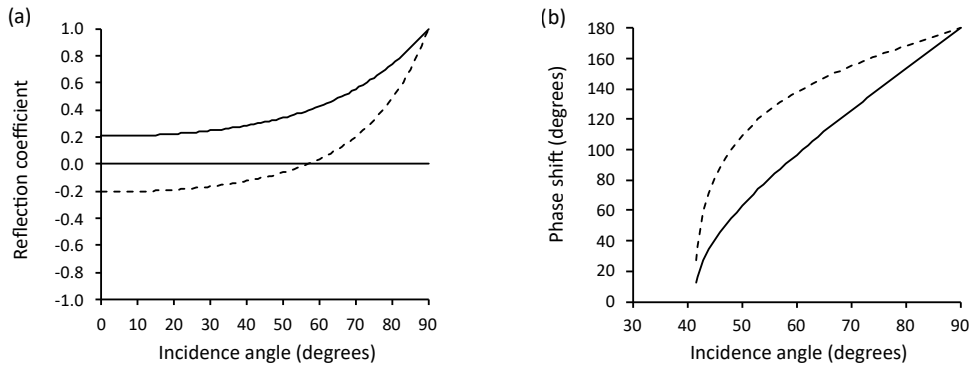

FIG. 9: (a) Reflection coefficients in partial external reflection ($n = 1.52$) for s-polarized light in total internal reflection (solid line) and p-polarized light (dashed line) as a function of the incidence angle. (b) Phase shifts in total internal reflection ($n = 1.52$) for s-polarized (solid line) and p-polarized (dashed line) light as a function of the incidence angle.

require wave polarization, only the dependence of the reflection coefficient on the angle of incidence. Thus, similar behavior could be observed, for example, with acoustic waves.[33]

The weak measurement technique, familiar from quantum mechanics, allows for the enhancement of small GH and IF shifts to such an extent that they can be measured with relatively modest experimental equipment, even in student laboratories. At the same time, the principle of weak measurement becomes more familiar and comprehensible, as it can also be explained classically. On the other hand, the quantum mechanical formulation clarifies many aspects related to these shifts, making it highly useful.

APPENDIX A: REFLECTION COEFFICIENTS AND PHASE SHIFTS.

In the partial external reflection the reflection coefficients $r_i(\theta) = R_i \exp(\phi_i(\theta))$ are real ($\phi_s = \phi_p = 0$) and for s and p polarized light they are given by (see Fig. 9(a))[1,34,35]

$$\begin{aligned} R_s &= -\frac{\cos(\theta) - n\sqrt{1-(1/n^2)\sin^2(\theta)}}{\cos(\theta) + n\sqrt{1-(1/n^2)\sin^2(\theta)}}, \\ R_p &= \frac{\sec(\theta) - n/\sqrt{1-(1/n^2)\sin^2(\theta)}}{\sec(\theta) + n/\sqrt{1-(1/n^2)\sin^2(\theta)}}, \end{aligned} \tag{A1}$$

where θ is the incidence angle of the beam. In the total internal reflection, the reflection coefficient are complex ($R_s = R_p = 1$) and the corresponding phase shifts are (see Fig. 9(b))

$$\begin{aligned} \phi_s &= 2\tan^{-1}\left(\sqrt{\frac{\cos^2(\theta_c)}{\cos^2(\theta)} - 1}\right), \\ \phi_p &= 2\tan^{-1}\left(\frac{1}{\sin^2(\theta_c)}\sqrt{\frac{\cos^2(\theta_c)}{\cos^2(\theta)} - 1}\right), \end{aligned} \tag{A2}$$

where θ_c is the the critical angle in the total internal reflection. Here $\theta_c = 41.14°$. The Eqs. (A1) and (A2) have various versions in literature depending on the used coordinate system. The versions shown here can be used directly with the shift equations presented in Section II.

APPENDIX B: OPTICAL COMPONENTS

We list here the essential optical components used in our experimental setup with approximate prices:

Component	**Thorlabs item**	**Price (USD)**	**Comment**
He-Ne laser	HNLS008L	1200	Any small power He-Ne laser can be used
Glan-Thompson polarizer	GTH5M	500	Glan-Taylor polarizer is another alternative
Small rotation mount	PRM05	250	
High precision rotation mount	PRM1	320	
Rotation stage	RP01	110	
Right-angle prism BK7	PS914	50	
Iris diaphragm	ID25	60	
Half-wave plate 633 nm	WPH05ME-633	280	
Quarter-wave plate 633 nm	WPQ05ME-633	280	
Digital camera IDS UI-1242		300	Any camera with 1280 x 1025 pixels

* Electronic address: tom.kuusela@utu.fi

[1] M. Born and E. Wolf, *Principles of Optics, 7th Edition*, page 52 (Cambridge University Press, Cambridge, 2024).

[2] J. D. Jackson, *Classical Electrodynamics, 3rd Edition*, page 306 (Wiley, Singapore, 2021).

[3] K. Y. Bliokh and A. Aiello,"Goos-Hänchen and Imbert-Fedorov beam shifts: an overview," J. Opt. **15**, 014001-1–16 (2013).

[4] M. R. Dennis and J. B. Götte,"The analogy between optical beam shifts and quantum weak measurements," New J. Phys. **14**, 073013-1–13 (2012).

[5] J. B. Götte and M. R. Dennis,"Generalized shifts and weak values for polarization components of reflected light beams," New. J. Phys. **14**, 073016-1–20 (2012).

[6] F. Goos and Hänchen,"Ein neuer und fundamentaler versucht zur totalreflexion," Ann. Phys., Lpz. **436**, 333–346 (1947).

[7] K. Artman,"Berechnung der seitenversetzung des totalreflektierten strahles," Ann. Phys., Lpz. **437**, 87–102 (1948).

[8] R. H. Renard,"Total reflection: a new evaluation of the Goos-Hänchen shift," J. Opt. Soc. Am. **54**, 1190–1197 (1964).

[9] C. Imbert,"Calculation and experimental proof of the transverse shift induced by total internal reflection of a circularly polarized light beam," Phys. Rev. D **5**, 787–798 (1972).

[10] M. Onoda, S. Murakami, and N. Nagaosa,"Hall effect of light," Phys. Rev. Lett. **93**, 083901-1–4 (2004).

[11] O. Hosten and P. Kwiat,"Observation of the spin Hall effect of light via weak measurements,"Science **319**, 787–790 (2008).

[12] A. Aiello and J. P. Woerdman,"Role of beam propagation in Goos-Hänchen and Imbert-Fedorov shift,"Opt. Lett. **13**, 1437–1439 (2008).

[13] F. Töppel, M. Ornigotti, and A. Aiello,"Goos-Hänchen and Imbert-Fedorov shifts from a quantum-mechanical perspective," New J. Phys. **15**, 113059-1–15 (2013).

[14] D. Stoler,"Operator methods in physical optics," J. Opt. Soc. Am. **71**, 334–341 (1981).

[15] Y. Aharonov, D. Z. Albert, L. Vaidman,"How the results of a measurement of a component of the spin of spin-1/2 particle can turn out to be 100," Phys. Rev. Lett. **60**, 1351–1354 (1988).

[16] I. M. Duck and P. M. Stevenson,"The sense in which a "weak measurement" of a spin-1/2 particle's spin component yields a value 100," Phys. Rev. D **40**, 2112–2117 (1989).

[17] N. W. M. Ritchie, H. G. Story, and R. G. Hulet,"Realization of a measurement of a "weak

value",” Phys. Rev. Lett. **66**, 1107-1110 (1991).

[18] G. Jayaswal, G. Misture, and M. Merano,“Observation of the Imbert-Fedorov effect via weak value amplification,” Opt. Lett. **39**, 2266–2269 (2014).

[19] Y. Qin, Y. Li, and Q. Gong,“Measurement of spin Hall effect of reflected light,” Opt. Lett. **34**, 2551–2553 (2009).

[20] G. Jayaswal, G. Misture, and M. Merano,“Observing angular deviations in light beam reflection via weak measurements,” Opt. Lett. **32**, 6257–6260 (2014).

[21] G. Jayaswal, G. Misture, and M. Merano,“Weak measurement of the Goos-Hänchen shift,” Opt. Lett. **82**, 1232–1234 (2013).

[22] A. Das and M. Pradhan,“Quantum weak measurement of Goos-Hänchen effect of light in total internal reflection using a Gaussian-mode laser beam,” Laser Phys. Lett. **17**, 066001-1–6 (2020).

[23] Y. Qin, Y. Li, Y.-F. Xiao, H. Yang, and Q. Gong,“Observation of the in-plane spin separation of light,”Opt. Express **19**,9636–9645 (2011).

[24] M. Merano, A. Aiello, G. W. van't Hooft, M. P. van Exter, E. R. Eliel, and J. P. Woordman,“Observation of Goos-Hänchen shifts in metallic reflection,” Opt. Express **15**, 15928–15934 (2007).

[25] M. Pfeifer and P. Fischer,“Weak value amplified optical activity measurement,” Opt. Express **17**, 16508–16517 (2011).

[26] F. Pillon, H. Gilles, S. Girard, and M. Laroche,“Goos-Hänchen and Imbert-Fedorov shifts for leaky guided modes,” J. Opt. Soc. Am. B **22**, 1290-1299 (2005).

[27] A. Aiello, M. Merano, and J. P. Woerdman,“Duality between spatial and angular shift in optical reflection,” Phys. Rev. A **80**, 061801-1–4 (2009).

[28] J. M. Ḿenard, A. E. Mattacchione, M. Betz, and H. M. van Driel,“Imaging the spin Hall effect of light inside semiconductors via absorption,” Opt. Lett. **34**, 2312-2314 (2009).

[29] I. V. Shadrivov, R. W. Ziolkowski, A. A. Zharov, and Y. S. Kivshar,“Excitation of guided waves in layered structures with negative refraction,” Opt. Express. **13**, 481–492 (2005).

[30] X.-H. Ling, H.-L. Luo, M. Tang, and S.-C. Wen,“Enhanced and tunable spin Hall effect of light upon reflection of one-dimensional photonic crystal with a defect layer,” Chin. Phys. Lett. **29**, 074209-1–4 (2012).

[31] C. Prajapati and D. Ranganathan,“Goos-Hänchen and Imbert-Fedorov shifts for Hermite-Gauss beams,” J. Opt. Soc. Am. A **29**, 1377-1382 (2012).

[32] N. Hermosa, A. Aiello, and J. P. Woerdman,"Radial mode dependence of optical beam shifts," Opt. Lett. **37**, 1044-1046 (2012).

[33] M. R. Dennis and J. B. Götte,"Scalar Goos-Hänchen shift for Robin boundary conditions," Proc. SPIE ed. E. J. Galvez, D. L. Andrews, and J. Glückstad **7950**, 79500J (2011).

[34] B. E. A. Saleh and M. C. Teich, *Fundamentals of Photonics 2nd Edition* (Wiley, New Jersey, 2007).

[35] I. R. Kenyon, *The Light Fantastic: A Modern Introduction to Classical and Quantum Optics* (Oxford University Press, New York, 2011).